NUCL SCI TECH (2016) 27:108
DOI 10.1007/s41365-016-0122-6

ALD-coated ultrathin Al_2O_3 film on $BiVO_4$ nanoparticles for efficient PEC water splitting

Guo-Liang Chang[1,2] · De-Gao Wang[2] · Yu-Ying Zhang[2] · Ali Aldalbahi[3] · Li-Hua Wang[2] · Qian Li[2] · Kun Wang[2]

Received: 17 May 2016 / Revised: 22 June 2016 / Accepted: 1 July 2016 / Published online: 25 August 2016

Abstract Bismuth vanadate ($BiVO_4$) is a promising semiconductor material for solar energy conversion via photoelectrochemical (PEC) water splitting, whereas its performance is limited by surface recombination due to trapping states. Herein, we developed a new method to passivate the trapping states on $BiVO_4$ surface using ultrathin aluminum oxide (Al_2O_3) overlayer by atomic layer deposition. The coated ultrathin Al_2O_3 film on $BiVO_4$ significantly enhanced photocurrent densities of the $BiVO_4$ anodes under standard illumination of AM 1.5 G (100 mW/cm^2). The electrochemical impedances and photoluminescence spectra were studied to confirm that the improved PEC water splitting performance of $BiVO_4$ was due to the decreased surface recombination state on $BiVO_4$, which effectively enhanced the charge separation.

Keywords Ultrathin Al_2O_3 overlayer · Photoelectrochemical water splitting · Surface state · Atomic layer deposition

This work was supported by the National Natural Science Foundation of China (21473236, 21227804), the Shanghai Municipal Commission for Science and Technology (13NM1402300) and the Chinese Academy of Sciences. Ali Aldalbahi acknowledges the support by the Deanship of Scientific Research, College of Science Research Center at King Saud University.

✉ Kun Wang
nanowangkun@sinap.ac.cn

[1] Department of Physics, College of Sciences, Shanghai University, Shanghai 200444, China

[2] Division of Physical Biology and Bioimaging Center, Shanghai Synchrotron Radiation Facility, CAS Key Laboratory of Interfacial Physics and Technology, Shanghai Institute of Applied Physics, Chinese Academy of Sciences, Shanghai 201800, China

[3] Chemistry Department, King Saud University, Riyadh 11451, Saudi Arabia

1 Introduction

Photoelectrochemical (PEC) water splitting offers the ability to convert solar energy into chemical energy by producing O_2 and H_2 gases [1, 2]. Bismuth vanadate ($BiVO_4$) has become a promising n-type semiconductor for PEC water splitting since 1999 when it was reported by Kudo et al. [3, 4] as a photocatalyst for water oxidation. Monoclinic scheelite $BiVO_4$ has high light absorption (bandgap, $E_g = 2.4$ eV), ample abundance, low toxicity and appropriate valence band position for O_2 evolution [3], but it suffers from poor electron transfer and collection in the photoelectrode, and sluggish water oxidation kinetics [3–5]. Efforts having been made to alleviate these restrictions include doping with nitrogen [6], introducing catalysts such as Co–Pi [7], p-type Co_3O_4 [8], NiOOH [9] and constructing nanostructures or heterojunctions [10–12]. The use of passivation layers has been an effective way to improve charge separation and transfer at semiconductor–liquid interfaces [13], for example, using Al_2O_3 [14] or TiO_2 [15, 16] and other nanomaterials [17–19] to passivate hematite, and NiO or CoO_x to passivate $BiVO_4$ [20, 21]. We developed a new method to passivate $BiVO_4$, in which atomic layer deposition (ALD) was utilized to deposit an ultrathin Al_2O_3 overlayer on $BiVO_4$ photoanodes, which perform much better in PEC water splitting.

2 Experimental

2.1 Preparation of $BiVO_4$ photoanode

Fluorine-doped tin oxide-coated glass substrates (FTO, TEC15, NSG) were seriatim cleaned with acetone, ethanol and deionized water. The mixed precursor (0.486 g bismuth nitrate pentahydrate, 1 mL acetylacetone and 0.273 g vanndyl acetylacetonate, from Sinopharm or Sigma-Aldrich) was dissolved in 20 mL acetic acid. The mixed precursor of 10 μL was dropped on to a FTO glass (available area 10 mm × 10 mm) by pipettor. After 30 min, the glass was heated in an air oven to 450 °C for 2 min and allowed to cool down in air. After repeating this procedure for five times, the sample was calcined in at 550 °C for 4 h. As the glass cooled down, a thin yellow film could be seen on the FTO glass. The ALD process used deionized water and $Al(CH_3)_3$ (trimethylaluminum) as precursors, and film thickness of Al_2O_3 could be controlled in angstrom scale. Typical pulse durations for trimethylaluminum and water were 0.05 and 0.03 s, respectively. After ALD depositing, the samples were heated in a furnace at 380 °C for 0.5 h to produce uniform and crystalline Al_2O_3 layer.

2.2 Material characterization

Morphologies of the samples were characterized with a scanning electron microscope (SEM JME2011, JEOL, Japan) and a high-resolution transmission electron microscope (HRTEM, FEI TECNAI G2 F20). TEM samples were prepared by scrapping the $BiVO_4$ film from the FTO glass with a new blade and transferring the powder carefully into an EP tube containing methanol (HPLC class). X-ray photoelectron spectra (XPS) were measured with a PerkinElmer 1257 model, operating at an average base pressure of $\sim 5.9 \times 10^{-9}$ Torr at 300 K with a non-monochromatized Al Kα line at 1486.6 eV and a hemispherical sector analyzer with resolution of 25 MeV.

2.3 Electrochemical characterization

The $BiVO_4$ photoanodes were fabricated by sealing the $BiVO_4$ electrodes (including the edges) with epoxy resin except for a 0.25-cm^2 square (unsealed) left for photoexcitation. An external Cu wire was connected to the FTO surface using a 63/37 Sn/Pb solder (Youbang Soldering Company, Hangzhou, China). An Autolab electrochemical station (Metrohm AG, Switzerland) equipped with a NOVA 1.8 software was employed to study electrochemical properties and stability of the as-fabricated photoanodes in a three-electrode electrochemical cell. The photoanodes were illuminated on the FTO side and tested.

2.4 PEC measurements

PEC activity of the samples was measured using line scan voltammetry in a standard three-electrode setup. $BiVO_4$ photoanode was regarded as the working electrode, a platinum plate as the counter electrode, and Ag/AgCl as the reference electrode. PBS (pH 7) was used as electrolyte in the measurements. The photocurrent density of each photoanode was recorded by the Autolab electrochemical station under the simulate light of 100 mW/cm^2 provided by a 500-W Xe lamp (Newport, Model SP 94023A) with an AM 1.5 G filter. The light intensity was standardized in advance using a calibrated silicon photodiode (Newport, 91150 V). The same lamp was used in photocurrent transient measurement. Electrochemical impedance spectra (EIS) were collected by the Autolab electrochemical workstation.

3 Results and discussion

The $BiVO_4$ photoanodes were prepared by dropping mixed precursor on FTO substrates; $BiVO_4$ nanoparticles were formed after crystallization. Ultrathin Al_2O_3 films were coated on $BiVO_4$ photoanodes via ALD process (Fig. 1a). SEM images in Fig. 1b, c show similar morphologies of $BiVO_4$ photoanodes before and after ALD process (5 cycles), indicating that ALD coating Al_2O_3 had little effect on the morphology of $BiVO_4$ photoanode. TEM images in Fig. 1d, e show that the $BiVO_4$ and $BiVO_4$·Al_2O_3 particles have an interlunar spacing of 0.309 nm, being well consistent with the JCPDS 75-2480, and the pristine and coated nanostructures do not differ from each other. According to Ref. [14], the 5-cycle Al_2O_3 is 0.75 nm thick (by spectroscopic ellipsometry on Si) and that is probably why the ALD treatment has little influence on the morphology and nanostructure of $BiVO_4$.

The electronic structure of $BiVO_4$ was checked by XPS (Fig. 2a–c). The pure $BiVO_4$ sample exhibited typical spin–orbit split of Bi $4f_{5/2}$ and Bi $4f_{7/2}$ signals, and V $2p_{1/2}$ and V $2p_{3/2}$ signals, in agreement with the literature [22, 23]. This confirms that the $BiVO_4$ sample prepared was identically the monoclinic scheelite $BiVO_4$. For the Al_2O_3-coated $BiVO_4$ sample, as shown in Fig. 2d, Al was detected, and a significant shift of O 1*s* peak can be seen in Fig. 2e, indicating two crystal structures in the sample. All these were consistent with the fact that the Al_2O_3 layer had covered the samples through ALD deposition.

PEC performance of the $BiVO_4$ photoanodes before and after the ALD process was investigated. As shown in

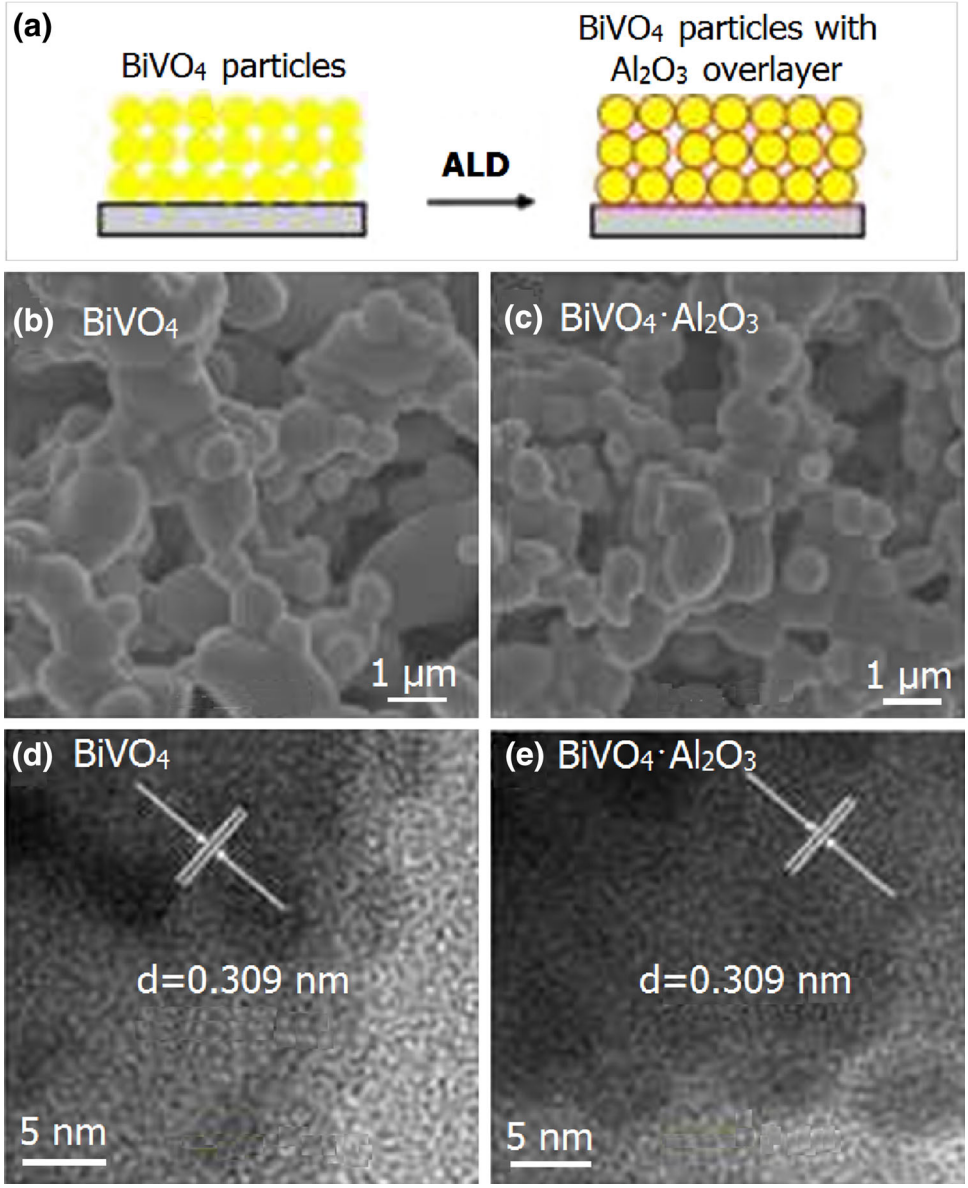

Fig. 1 Schematic illustration of preparing Al_2O_3-coated $BiVO_4$ particles (**a**), *top-view* SEM images of the pristine and Al_2O_3-coated $BiVO_4$ photoanode (5 cycles) (**b**, **c**), and TEM images of the pristine and Al_2O_3-coated $BiVO_4$ (5 cycles) (**d**, **e**)

Fig. 3a, the photocurrent densities of Al_2O_3-coated $BiVO_4$ photoanodes were significantly higher than the pristine. In particular, the photocurrent density of $BiVO_4{\cdot}Al_2O_3$ photoanode by 5 ALD cycles reached over 1.0 mA/cm^2 at 1.23 V versus RHE under the standard illumination of AM 1.5 G (100 mW/cm^2), which was twice of the pristine one's. It confirms that Al_2O_3 overlayer deposition can strongly enhance the PEC performance of $BiVO_4$ photoanodes. Yet, when by further increasing the ALD cycles to 10 ALD cycles, the photocurrent density decreased, partly because of the large increased resistance in the Al_2O_3 overlayer. In fact, the Al_2O_3-coating was optimized at 5 ALD cycles..

Photocurrent transient measurement was performed to assess the charge recombination at the sample/electrolyte interface. The measurement was taken under curtain bias potential, and the time-resolved photocurrent was recorded, while the illumination was turned on and off, with the $BiVO_4{\cdot}Al_2O_3$ sample of 5 ALD cycles. As shown in Fig. 3b, c, the $BiVO_4{\cdot}Al_2O_3$ sample at 0.5 and 0.9 V versus RHE has much smaller current spikes than those of the pristine $BiVO_4$ photoanode. According to Ref. [14], the appearance of sharp spike is mainly because that photogenerated holes accumulate at the interface or oxidize the trap states on the semiconductor surface and in the bulk. A larger bias potential allows the holes to cross over the interface more easily to oxidize water. And, the motion of holes reduces the anodic current. In our experiment, the anodic current spike at 0.5 V versus RHE is much higher than that at 0.9 V versus RHE. After the ALD treatment,

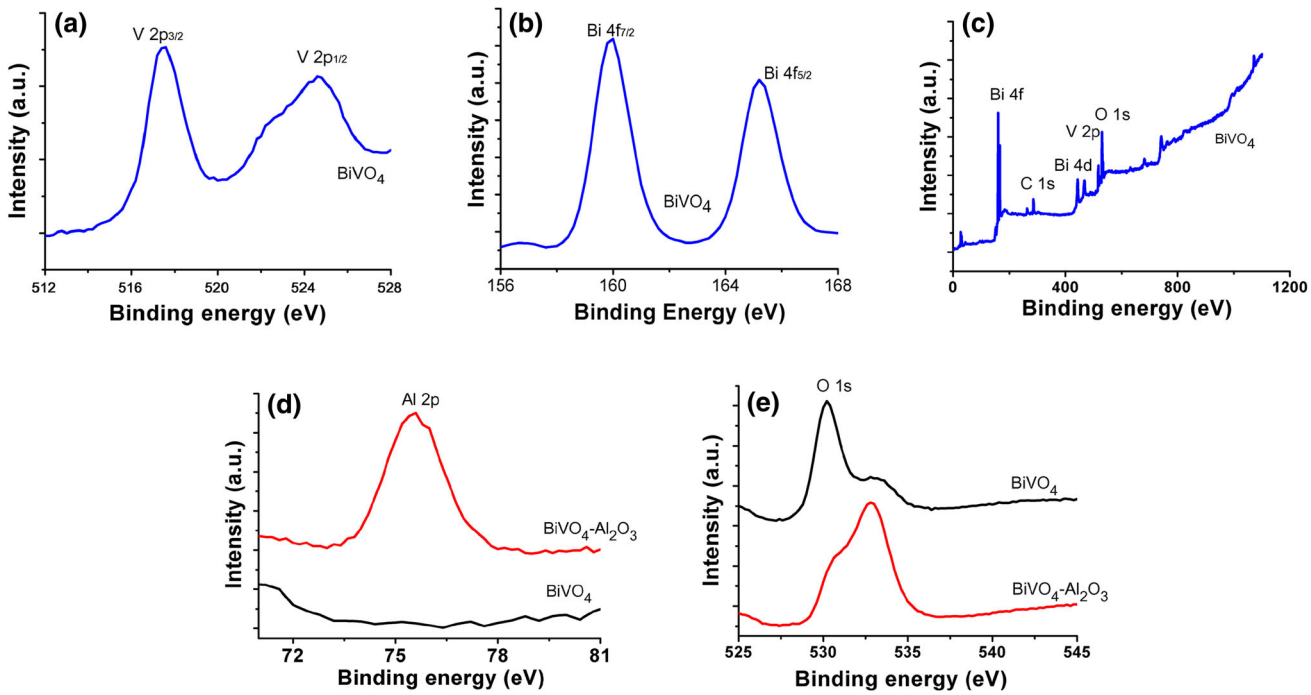

Fig. 2 X-ray photoelectron spectra of the pristine $BiVO_4$ sample (**a**–**c**) and the Al_2O_3-coated $BiVO_4$ sample (**d**, **e**)

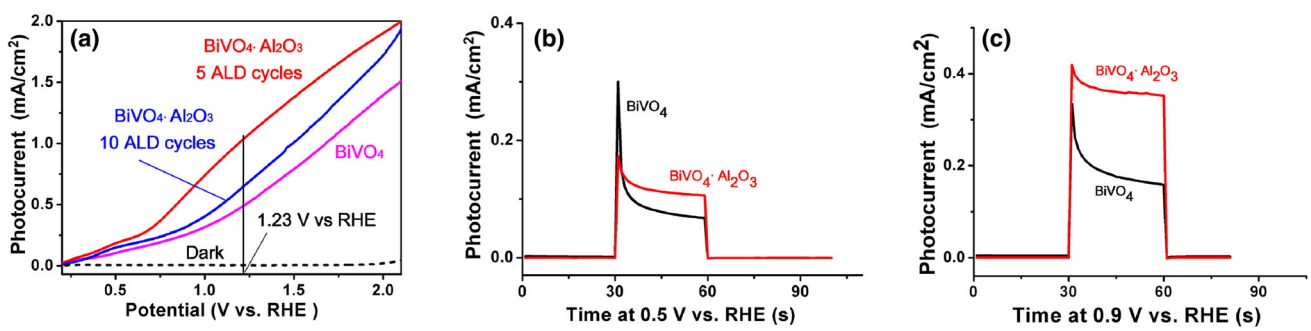

Fig. 3 Photocurrent densities of Al_2O_3-coated $BiVO_4$ photoanodes under simulated solar illumination (**a**) and, light chopping photocurrent densities at 0.5 (**b**) and 0.9 (**c**) V versus RHE, for $BiVO_4$ photoanodes before and after 5-cycle Al_2O_3 deposition

the current spikes became smaller and much smoother. This suggests that the charge recombination on the surface of $BiVO_4$ photoanode may be passivated after depositing the ultrathin Al_2O_3 overlayer.

To better support this hypothesis, photoluminescence (PL) of the Al_2O_3-coated $BiVO_4$ sample (5 cycles) was studied. PL spectroscopy is an effective technique to study separation efficiency of the photogenerated carriers. The higher PL intensity indicates the bigger probability of charge recombination [24]. Figure 4 shows the PL quantum yield of the Al_2O_3-coated $BiVO_4$ photoanode was smaller than the pristine one, indicating that the charge recombination in $BiVO_4$ photoanode was effectively inhibited after the Al_2O_3 coating [8]. Therefore, the ultrathin Al_2O_3 overlayer can effectively passivate the charge recombination on the surface of $BiVO_4$ photoanodes.

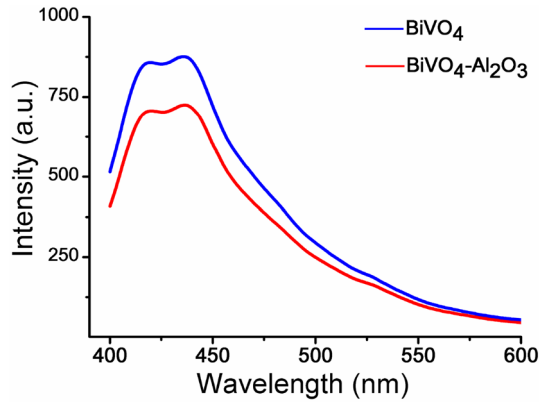

Fig. 4 The PL emission spectra of $BiVO_4$ photoanode before and after Al_2O_3 deposition (5 cycles)

Also, electrochemical impedance spectroscopy (EIS) was performed with the samples covered with 5 ALD cycles Al_2O_3 and the control (without Al_2O_3 overlayer). Here, we used an equivalent circuit consisted of 2 RC elements in series, accounting for semiconductor behavior and surface processes, as shown in Fig. 5a [14, 25].

In Fig. 5b, space charge resistances (R_{SC}) of the samples before and after ALD treatment are all stable around 10^3 Ω, but a remarkable decrease in charge transfer resistances (R_{CT}) can be seen after ALD treatment (Fig. 5c). The R_{CT} decrease could lead to a reduction of overpotential, hence the increase in photocurrent we observed. Yet it will be much clearer to reveal the effect of Al_2O_3 layer, when we look into the change in Helmholtz capacitance (C_H) or space charge capacitance (C_{SC}) after ALD treatment (Fig. 5d, e). The C_{SC} increased and C_H decreased as a result of Al_2O_3 coating. As capacitance is the charge over voltage, so the C_H decrease after the ALD treatment may be related to the change in voltage or charge distribution at the sample/electrolyte interface. In this experiment, the C_H decrease is due to the decreased free charge density in surface trap states because of the passivation of surface states. Another reason is that the relatively high dielectric of Al_2O_3 layer may improve the charge screening of anions in Helmholts layer [14]. On the other hand, as shown in Fig. 5d, after ALD treatment, the space charge capacitance (C_{SC}) increased significantly in the entire range of potential bias applied. According to Ref. [14], this can be explained as follows: in order to balance the applied voltage, charges are extracted more from the space charge layer than before due to the decrease in surface states, leading to charge increase in the space charge region [14], i.e., the significant increase of C_{SC}. Therefore, we can conclude that the Al_2O_3 overlayer brought about a significant decrease in the charge density on the surface (surface states), and better performance of the $BiVO_4$ photoanode.

4 Conclusion

In summary, ALD coating ultrathin Al_2O_3 overlayer can effectively enhance the PEC water splitting performance of $BiVO_4$ photoanodes. Particularly, 5 ALD cycles Al_2O_3 deposition increased the photocurrent density of $BiVO_4$ photoanode from ~0.5 to ~1.0 mA/cm^2, at 1.23 V versus RHE under the standard illumination (100 mW/cm^2). In transient photocurrent measurement, the anodic current spikes of the sample became much smoother after depositing Al_2O_3 overlayer. In photoluminescence spectra, the photoluminescence quantum yield of the Al_2O_3-coated $BiVO_4$ photoanode was smaller than the pristine one. And in electrochemical impedance measurement, the charge transfer resistance and capacitance of Al_2O_3-coated sample differed significantly from the pristine. All of these provide convincing evidence that Al_2O_3 overlayer successfully passivates the surface trap states of $BiVO_4$, thus inhibits charge recombination and benifits the performance of $BiVO_4$. Though the stability of Al_2O_3-coated $BiVO_4$ in

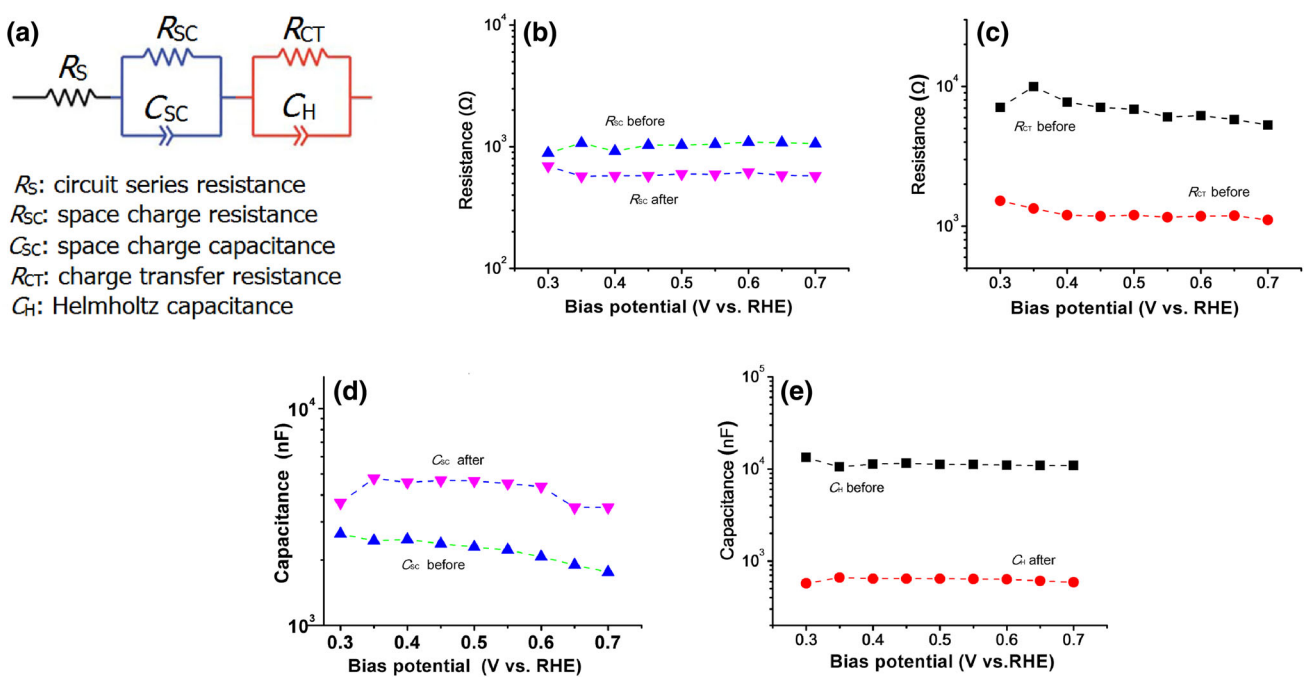

Fig. 5 Electronic equivalent circuit **a** signing the photoanode/electrolyte system in our EIS measurement before and after 5 ALD cycles of Al_2O_3, the space charge and charge transfer resistances (**b**, **c**), and the space charge and Helmholtz capacitances (**d**, **e**)

electrolyte (PBS) was not as good as expected, it still provides a promising approach to passivate $BiVO_4$, and thus improve the performance of $BiVO_4$ for efficient photoelectrochemical water splitting.

References

1. A. Fujishima, K. Honda, Electrochemical photolysis of water at a semiconductor electrode. Nature **238**, 37–38 (1972). doi:10.1038/238037a0
2. M. Grätzel, Photoelectrochemical cells. Nature **414**, 338–344 (2001). doi:10.1038/35104607
3. Y. Park, K.J. McDonald et al., Progress in bismuth vanadate photoanodes for use in solar water oxidation. Chem. Soc. Rev. **42**(6), 2321–2337 (2013). doi:10.1039/C2CS35260E
4. A. Kudo, K. Omori, H. Kato, A novel aqueous process for preparation of crystal form-controlled and highly crystalline $BiVO_4$ powder from layered vanadates at room temperature and its photocatalytic and photophysical properties. J. Am. Chem. Soc. **121**(49), 11459–11467 (1999). doi:10.1021/ja992541y
5. J.A. Seabold, K.S. Choi, Efficient and stable photo-oxidation of water by a bismuth vanadate photoanode coupled with an iron oxyhydroxide oxygen evolution catalyst. J. Am. Chem. Soc. **134**(4), 2186–2192 (2012). doi:10.1021/ja209001d
6. T.W. Kim, Y. Ping, G.A. Galli et al., Simultaneous enhancements in photon absorption and charge transport of bismuth vanadate photoanodes for solar water splitting. Nat. Commun. **6**, 8769 (2015). doi:10.1038/ncomms9769
7. M. Zhou, J. Bao, W.T. Bi et al., Efficient water splitting via a heteroepitaxial $BiVO_4$ photoelectrode decorated with Co–Pi catalysts. Chem. Sus. Chem. **5**(8), 1420–1425 (2012). doi:10.1002/cssc.201200287
8. X.X. Chang, T. Wang, P. Zhang et al., Enhanced surface reaction kinetics and charge separation of p–n heterojunction Co_3O_4/$BiVO_4$ photoanodes. J. Am. Chem. Soc. **137**(26), 8356–8359 (2015). doi:10.1021/jacs.5b04186
9. T.W. Kim, K.S. Choi, Nanoporous $BiVO_4$ photoanodes with dual-layer oxygen evolution catalysts for solar water splitting. Science **343**(6174), 990–994 (2014). doi:10.1126/science.1246913
10. R. Saito, Y. Miseki, K. Sayama, Highly efficient photoelectrochemical water splitting using a thin film photoanode of $BiVO_4$/SnO_2/WO_3 multi-composite in a carbonate electrolyte. Chem. Commun. **48**(32), 3833–3835 (2012). doi:10.1039/C2CC30713H
11. X.J. Shi, I.Y. Choi, K. Zhang et al., Efficient photoelectrochemical hydrogen production from bismuth vanadate-decorated tungsten trioxide helix nanostructures. Nat. Commun. **5**, 4775 (2014). doi:10.1038/ncomms5775
12. L.W. Zhang, E. Reisner, J.J. Baumberg, Al-doped ZnO inverse opal networks as efficient electron collectors in $BiVO_4$ photoanodes for solar water oxidation. Energy Environ. Sci. **7**(4), 1402–1408 (2014). doi:10.1039/C3EE44031A
13. R. Liu, J. Spurgeon, X.G. Yang, Enhanced photoelectrochemical water-splitting performance of semiconductors by surface passivation layers. Energy Environ. Sci. **7**, 2504–2517 (2014). doi:10.1039/C4EE00450G
14. F.L. Formal, N. Tétreault, M. Cornuz et al., Passivating surface states on water splitting hematite photoanodes with alumina overlayers. Chem. Sci. **2**, 737–743 (2011). doi:10.1039/c0sc00578a
15. X.G. Yang, R. Liu, C. Du et al., Improving hematite-based photoelectrochemical water splitting with ultrathin TiO_2 by atomic layer deposition. ACS Appl. Mater. Interfaces **6**(15), 12005–12022 (2014). doi:10.1021/am500948
16. P. Wang, D. Wang, C. Peng, C. Fan, TiO_2 nanorod arrays of a high photo-to-hydrogen efficiency for photoelectrochemical water decomposition. Nucl. Tech. **35**, 472–476 (2012). doi:10.11889/j.0253-3219.2012.hjs.35.472
17. Y. Zhang, T. Tian, Y. Sun, Y. Zhu, Q. Huang, The biocatalytic activity of inorganic nanomaterials. Chin. Sci. Bull. **59**, 158–168 (2014). doi:10.1360/972013-311
18. M. Liu, K. Wang, N. Chen, L. Wang, Radiotherapy enhancement with gold nanoparticles. Nucl. Tech. **38**, 090501–090506 (2015). doi:10.11889/j.0253-3219.2015.hjs.38.090501. **(in Chinese)**
19. D. Zhu, X. Zuo, C. Fan, Fabrication of nanometer-sized gold flower microelectrodes for electrochemical biosensing applications. Sci. Sin. Chim. **45**, 1214–1219 (2015). doi:10.1360/N032015-00039
20. M. Zhong, T. Hisatom, Y.B. Kuang et al., Surface modification of CoO_x loaded $BiVO_4$ photoanodes with ultrathin p-type NiO layers for improved solar water oxidation. J. Am. Chem. Soc. **137**(15), 5053–5060 (2015). doi:10.1021/jacs.5b00256
21. M.F. Lichterman, M.R. Shaner, S.G. Handler et al., Enhanced stability and activity for water oxidation in alkaline media with bismuth vanadate photoelectrodes modified with a cobalt oxide catalytic layer produced by atomic layer deposition. J. Phys. Chem. Lett. **4**(23), 4188–4191 (2013). doi:10.1021/jz4022415
22. K. Hirota, G. Komatsu, M. Yamashita et al., Formation, characterization and sintering of alkoxy-derived bismuth vanadate. Mater. Res. Bull. **27**(7), 823–830 (1992). doi:10.1016/0025-5408(92)90177-2
23. M.C. Long, W.M. Cai, J. Cai et al., Correlation of electronic structures and crystal structures with photocatalytic properties of undoped, N-doped and I-doped TiO_2. Chem. Phys. Lett. **40**(1–3), 71–76 (2006). doi:10.1016/j.cplett.2005.12.036
24. D.K. Ma, M.L. Guan, S.S. Liu et al., Controlled synthesis of olive-shaped Bi_2S_3/$BiVO_4$ microspheres through a limited chemical conversion route and enhanced visible-light-responding photocatalytic activity. Dalton Trans. **41**(18), 5581–5586 (2012). doi:10.1039/C2DT30099K
25. J. Wielant, V. Goossens, R. Hausbrand et al., Electronic properties of thermally formed thin iron oxide films. Electrochim. Acta **52**(27), 7617–7625 (2007). doi:10.1016/j.electacta.2006.12.041